東京大学大学院新領域創成科学研究科
環境学研究系自然環境学専攻
自然環境構造学分野

平成 18 年度　修士論文

正規化植生指標 (NDVI) を用いた アムール川流域における 土地被覆変化の評価

Evaluation of land-cover change in Amur basin using NDVI derived from NOAA/AVHRR PAL dataset

2007 年 1 月 31 日提出

2007 年 3 月修了

指導教員　春山成子　助教授

学籍番号　56726　増田佳孝

Contents

Contents of diagram

Ⅰ. Background of study

The Amur River is an international river with a total length of 4350 km and a huge drainage area of 2,051,500 km^2. Its upstream region is in Mongolia, which has a steppe climate (Köppen's Bs world climate zone). Its midstream and downstream regions flow through China and the vicinity of the Russian border, which lies in the cool-temperate zone with low winter rainfall (Dw zone).

Recently, environmental changes originating in the land-cover change have been occurring in the Amur River basin. For instance, the wetland habitat of the crane has been shrinking because of land development, increased sedimentation of rivers through the development of arable land, increased chemical loading of rivers through the expansion of agricultural activity, and air pollution due to forest fires.

In particular, the agriculture has been developed by Chinese government and the cultivated area has been increased in these 20 years in Heilongjiang Province[1)], and the area has changed into an important food production region[2)].

In contrast, the Russian territory through which the river passes has been in a state of economic depression since the collapse of the old Soviet federation. Therefore, the regional differences in land-cover change in the Amur River basin are great. An objective evaluation of the factors influencing anthropogenic land-cover change in the basin is needed [3)]. The only research data that we have on land-use and land-cover change in the area is the results of statistical material analyses of individual regions [4)]. There has been no research on the entire Amur River basin; nor has there been any research on secular variations in land cover.

I therefore performed satellite remote-sensing research on the secular variations in land cover over the entire Amur River basin. By using the NDVI (Normalized Difference Vegetation Index), I aimed to pinpoint regions that are experiencing marked land-cover changes and to explain the trends in these changes.

Ⅱ. Outline of study area

The Amur River basin is located at lat 41.42°–55.56°N and long 107.32°–141.70°E. The direction of the flow of the Amur River changes as the river courses from midstream to downstream to the east. The river is joined by the Ussuri River which flows from south to north around Khabarovsk, and by the Songhua River which flows from southwest to northeast around Sanjiang Plain (Figure 1).

Structural geographical changes are seen in the Amur River basin as the river flows from west to east. The mountainous district more than 1000 m above sea level (asl) extends to the west, and plains where the altitude is below 100 m spread out around Sanjiang plain (Figure 2).

Peat wetlands are distributed in the floodplains and on the plains of the valley bottoms in the hilly country south of the Amur River. Agricultural activity is active in the eastern Amur River basin. However, the climate is very cold: in the city of Harbin the annual mean temperature is 4.6 °C, and the temperature in January is –20 °C [5] (Figure 3). The monthly mean temperature in July is 25 °C, and rainfall is concentrated in summer. Only one crop is planted each year in the Amur River basin[6].

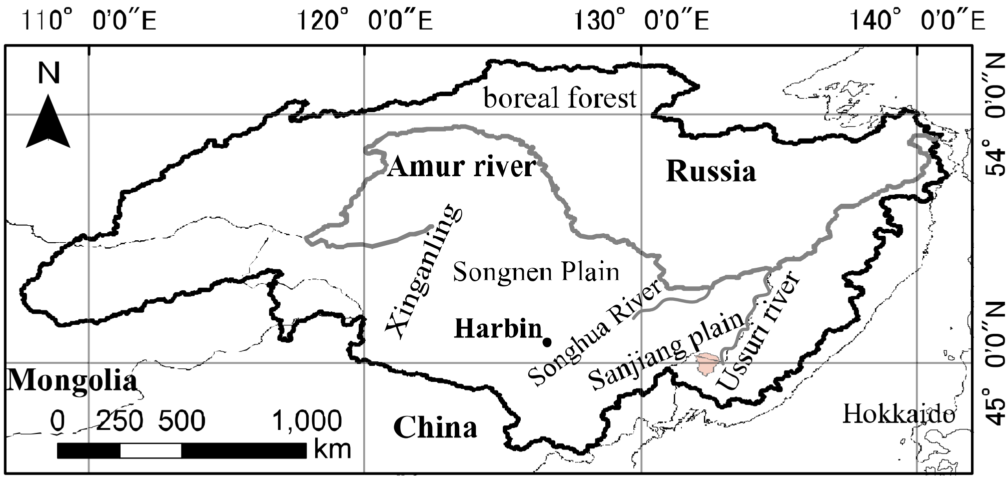

Figure 1. Amur River basin

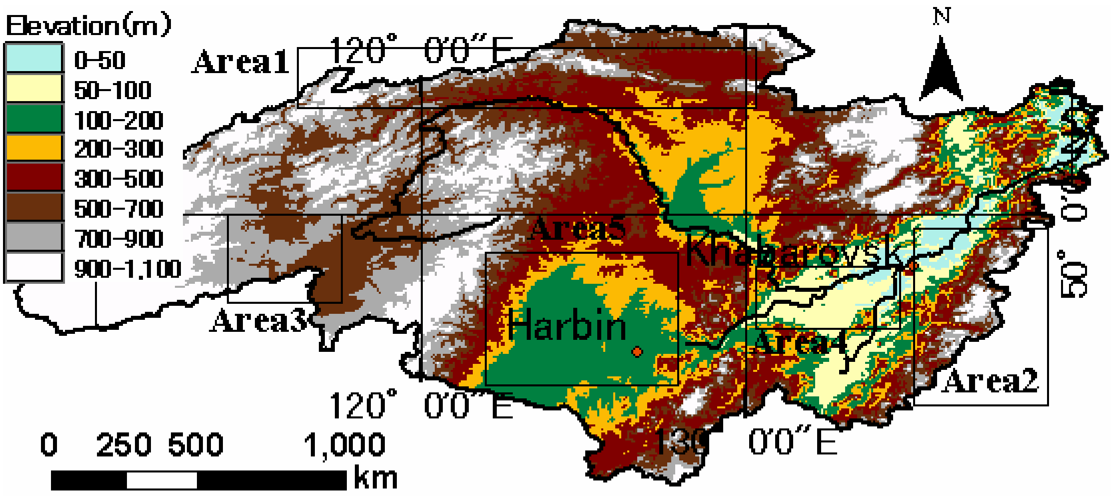

Figure 2. Elevation map of Amur river basin

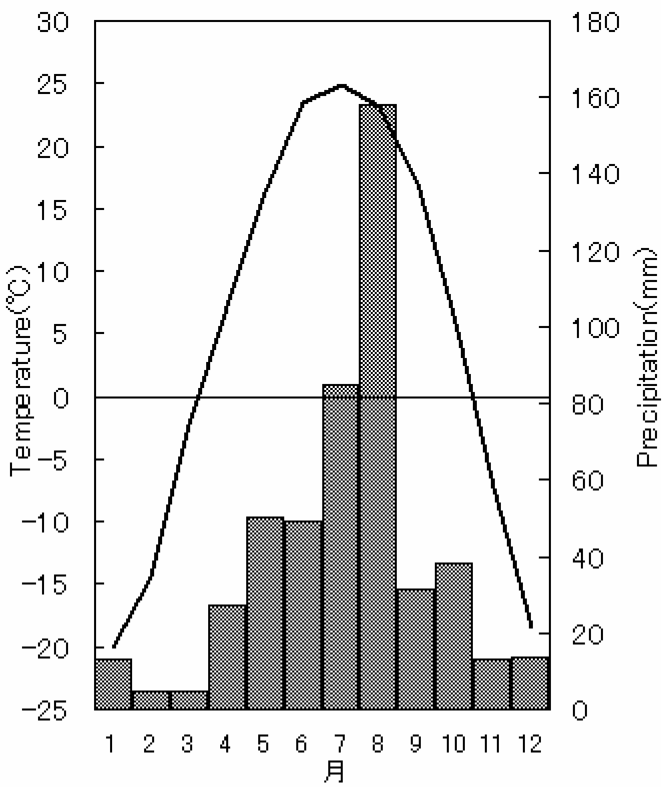

Figure 3. Temperature and precipitation in Harbin city in 2000

Ⅲ. Data used

1. NOAA/AVHRR PAL Dataset (PAL data)

Pathfinder AVHRR(Advanced Very High Resolution Radiometer) Land (PAL) data offered by the DAAC (Data Active Archive Center) of NASA/GSFC (National Aeronautics and Space Administration / Goddard Space Flight Center) was used to analyze land-cover changes in the Amur basin. The PAL dataset was collected by the AVHRR sensor installed on the NOAA (National Oceanic and Atmospheric Administration) weather satellite（Figure 4）. The AVHRR sensor measures emitted and reflected radiation in five channels (bands) of the electromagnetic spectrum; *Ch* (channel). 1 (visible light, 0.58 to 0.68 micrometer), *Ch.* 2 (near-infrared rays, 0.725 to 1.1 micrometer), *Ch.* 3 (mid-infrared rays, 3.55 to 3.93 micrometer), *Ch.* 4, *Ch.* 5 (heat infrared rays, 10.5 to 11.5 micrometer, 11.5 to 12.5 micrometer) are included. The mid-infrared band is used for sea surface temperature mapping and is not available in the PAL data.

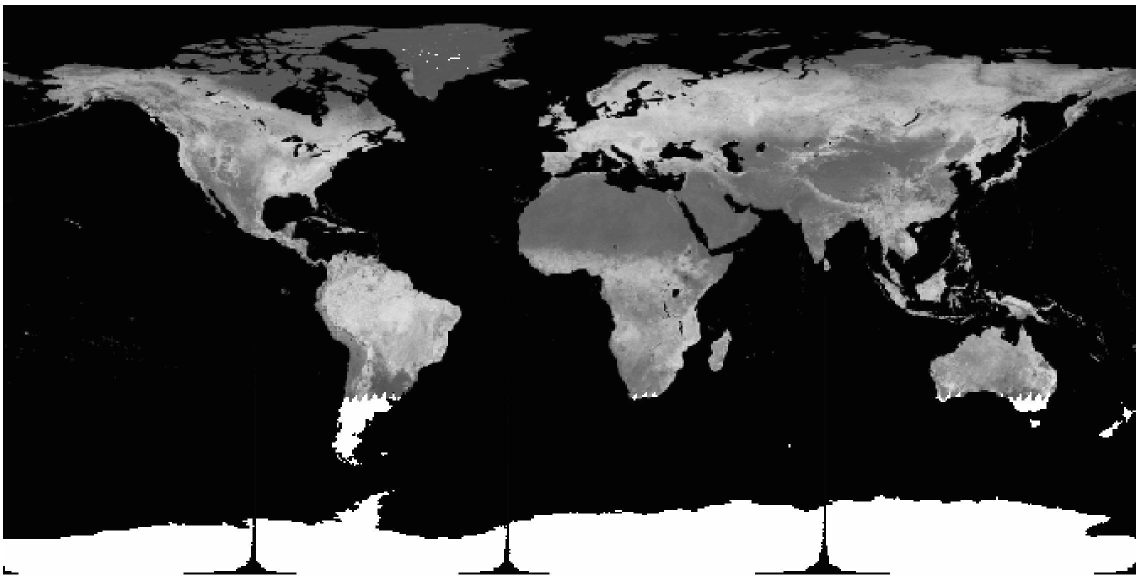

Figure 4. NOAA/AVHRR PAL data

（PAL NDVI data converted to the equal angular projection from the Goode Interrupt Homolosine Projection）

The first AVHRR channel is located in a part of the spectrum where chlorophyll in leaves causes considerable absorption of incoming radiation, and the second channel is in a region where the spongy mesophyll leaf structure leads to considerable reflectance. The radiances from channels 4 and 5 depend on the surface temperature. Therefore, by converting the radiance to brightness temperature, an approximation of the surface temperature will be obtained.

PAL data from July 1981 are available and can be analyzed from 1982 to 2000 to use the whole year data. Moreover, because PAL data are collected globally, the entire Amur River basin could be analyzed: this is why this dataset was the most suitable for the study.

The data divided the year into 36 seasons. The 10-day composite data provided by the PAL data removes the effects of clouds by choosing the observations on the day that has the highest NDVI value. Therefore the 10-day PAL data can provide the surface observations under near-clear sky condition.

The Goode Interrupt Homolosine Projection used by the PAL data has to be converted to the equal angular projection so that the latitudes and longitudes of pixels can be determined. Therefore, the spatial resolution is converted from 8km into 0.1° (about 10 km) of both latitude and longitude with the tool that the homepage offered (http://daac.gsfc.nasa.gov).

The NDVI relates to the density and active growth of green plants, and it can be calculated from differences in the spectral reflection of chlorophyll in the visible light and near-infrared ranges[7]. NDVI is the ratio, which has been shown to be highly correlated with vegetation parameters such as land cover[8], green-leaf leaf area index (LAI)[9], and green-leaf biomass[10], hence, is of considerable value for vegetation discrimination.

Like the above mentioned the first AVHRR channel is in a part of the spectrum where chlorophyll causes considerable absorption of incoming radiation and the second channel is in a spectral region where spongy mesophyll leaf structure leads to considerable reflectance. In a word, vegetation strongly absorbs wavelength of visible red. On the other hand, the light of the wavelength of the near infrared rays reflects strongly. This difference is a feature not seen so much in other land cover. If this difference is used, distinguishing the vegetation from other land covers becomes possible. For the reasons like the above-mentioned, NDVI is widely used for the observation and evaluation of vegetation and the most famous vegetation index.

In PAL data, NDVI is calculated by the following formula.

$$NDVI = \frac{Ch.2 - Ch.1}{Ch.2 + Ch.1}$$

The NDVI equation produces values in the range of 1.0 to -1.0, where increasing positive values indicate increasing green vegetation and the negative values indicate non-vegetated surface features such as water, barren land, ice, and snow.

2. Statistical materials used in the agricultural and field investigation

The amount of land in Heilongjiang Province transformed for irrigation between 1980 and 2000 was determined from the Heilongjiang Province statistical yearbook (2001). Moreover, the area sown to the main commercial crops (Rice, wheat, corn and soybean) between 1978 and 2000 and the patterns of transition of production were determined from the statistical material[11]. And also transition of total cultivated area, rice field and upland field in Heilongjiang Province was determined. In September 2005 I performed a field investigation in which I used GPS and digital cameras to observe and record the land cover in the Sanjiang plain, the Songnen Plain and around Khabarovsk Krai（Figure 5,6）.

The observation point and the migration pathway in field investigation were showed in Figure 5. The location information was obtained by the GPS receiver made by the Germin company. A red line in figure shows the track (the passed place) and a blue point shows the way point (the place where vegetation was recorded.).

The photographs in the field observation were showed in Figure 6. Figure 1-7 corresponds to blue point 1-7 shown in Fig.5. The position in which each photograph had been taken was summarized in the table. Fig.6-1 is Salt marsh. The surrounding is being modified to a corn field and industrial ground. Fig.6-2 is Harbin City. The construction rush of a large-scale building is seen. The left is Songhua river. Figure6-3 is wetland. Some types exist also in the wetland. The wetland vegetation in waterside and left from the waterside is different around Area.4. Most of the wetland was converted to the farmland around Area.4 recently. Figure 6-4 is the confluence part of Amur River and Songhua River. Right turbid water is Songhua River from China. It is guessed that a large amount of sediment flows in the Songhua river because of the land development in China. Figure6-5 is the cornfields. There are artificial modifications to Cornfields in hill around Area.5. The original forest in the hill is almost deforested as shown in the photograph. Figure6-6 is rice fields. Floodplains were being used for them. In the center of the photograph, there is irrigation equipment. Figure6-7 is the soybean fields. Hillside terraces were being used for them.

These information was used to consider the result of PAL data analysis.

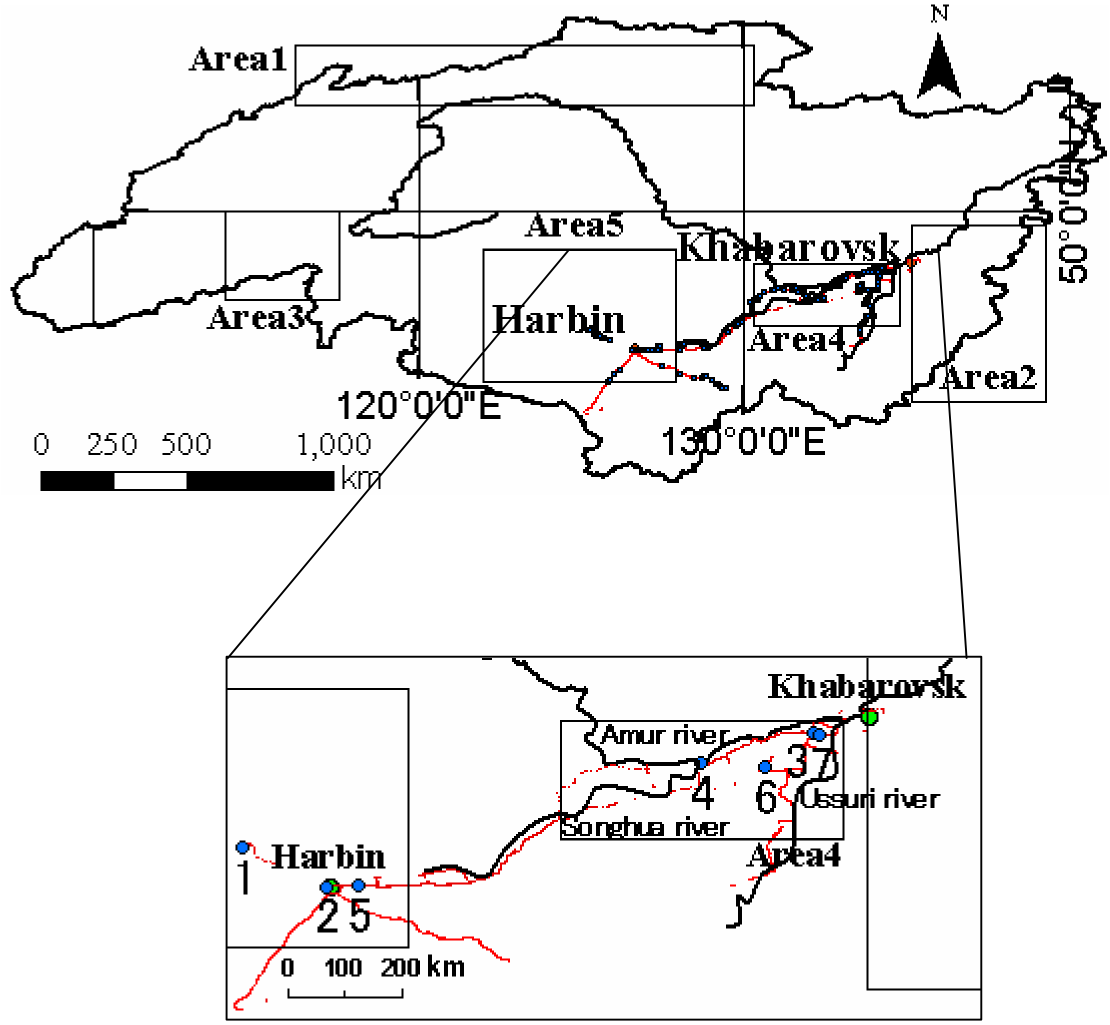

Figure 5. The observation point and the migration pathway in field investigation

(The location information was obtained by the GPS receiver made by the Germin company. A red line in figure shows the track and a blue point shows the photo point. The photograph in point 1-7 is shown in Fig.6.)

Fig.6-1. Salt marsh (The surrounding is being modified to a corn field and industrial ground.)

Fig.6-5. Cornfields (Artificial modification to Cornfields in hill around Area.5)

Fig.6-2. Harbin City (The construction rush of a large-scale building is seen. The left is Songhua river.)

Fig.6-6. Rice fields (Floodplains were being used. In the center of the photograph, there is irrigation equipment.)

Fig.6-3. Wetlands (Most of the wetland was converted to the farmland around Area.4)

Fig.6-7. Soybean fields (Hillside terraces were being used)

Fig.6-4. Confluence part of Amur River and Songhua River. (Right turbid water is Songhua River from China.)

GPS data information on point 1-7

Point	Latitude	Longitude	LandUse
1	46.386	125.254	salt marsh
2	45.758	126.586	Harbin city
3	48.194	134.27	wetland
4	47.704	132.511	river
5	45.769	127.098	corn
6	47.627	133.51	rice
7	48.151	134.375	soybean

Figure 6. Photograph in field investigation

3. CRU TS2.0

As for the influence on the land cover, both a natural factor and the human factor should be thought. Then, to catch a climatic change, the Climate Research Unit (CRU) time series (TS) data-set 2.0 was used. The data is supplied on a 0.5 degree grid, covering the global land surface. The data grid is envisaged as a rectangle with boundaries at the poles and the International Date Line. Data is only supplied for land boxes on the grid, which total 67420. There are five climatic variables available: cloud cover, diurnal temperature range (DTR), precipitation, temperature and vapor pressure. The data is supplied at a monthly time-step for 1901-2100. To clarify the climatic change in the Amur river basin, precipitation and temperature data were used from among this. And, some climatic trends concerning precipitation and temperature were analyzed.

Secular variation in mean temperature at each month from 1982-2000, secular variation in annual mean temperature from 1961-1990 and 1982-2000, secular variation in monthly precipitation from 1982-2000, secular variation in yearly precipitation from 1961-1990 and 1982-2000 were analyzed. The purpose of the trend analysis from 1961 to 1990 is to catch a more long-term climatic change.

Ⅳ. Method of study

1. Analysis of secular variation from 1982 to 2000

I used the technique proposed in 2004 by Kondoh to analyze the global-scale vegetation and land-cover changes from 1982 to 2000 from the PAL data [12] and to thus clarify the land-cover changes over the entire Amur River basin. Coordinates were given to the image by geometric collection. The following four parameters were used for the analysis: sum of NDVI (ΣNDVI) during the year; maximum NDVI ($NDVI_{max}$), standard deviation ($NDVI_{std}$) of ΣNDVI; and the trajectory on the Ts (surface temperature)–NDVI scatter chart (TRJ) [13]. The flow chart in Figure 3 was used for PAL data analysis.

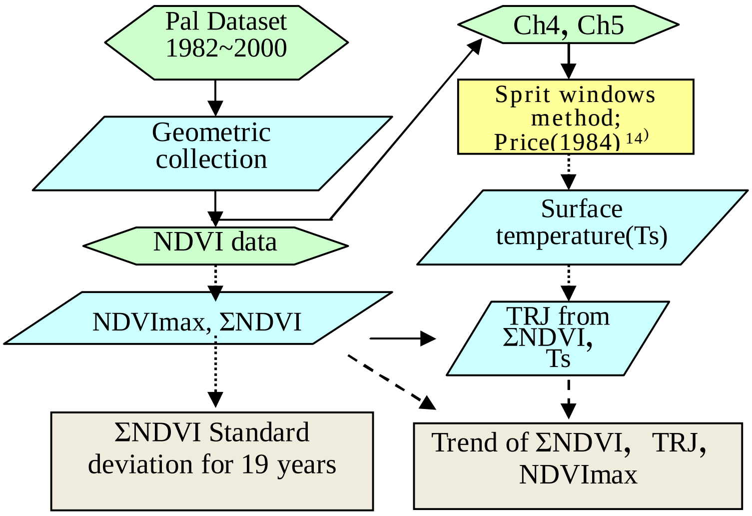

Figure 7. Flow chart of PAL data analysis

(The solid line shows the work flow. The dotted line shows the calculation by the program. The broken line shows the trend analysis of 19 years by the program.

With two channels *(Ch4, Ch5)* of the heat infrared rays, the split window method of Price (1984) was used to calculate the surface temperature[14] . Therefore, the influence of the atmosphere is almost corrected. Ts was calculated by the following formula $Ts = Ch.4 + 3.3 \times (Ch.4 - Ch.5)$)

$NDVI_{max}$ is used as an index related to the maximum LAI or the maximum biomass. It is verified that the vegetation index is associated with LAI and the biomass after the launch the first of 1972 Landsat by a lot of researches. Therefore, maximum NDVI of a certain year is sure to correspond to maximum LAI or the maximum biomass in the year. This parameter has already been used by Kondoh (2004). Then, the maximum value of NDVI was extracted every year, and the trend of 19 years at an analytical period was examined.

ΣNDVI is an index that corresponds to the biomass each year. It is clarified that the ΣNDVI relates to the biomass by Gowardet al.(1985)[15] and Boxet al.(1989)[10]. ΣNDVI was calculated by the following formula.

$$\sum NDVI = \sum_{i=1}^{N} a_i$$

Variable a_i shows a NDVI value of a season. As a threshold between vegetated and non-vegetated, the commonly used value of NDVI = 0.1 was applied[12]. Pixels whose NDVI is lower than 0.1 are judged as non-vegetated regions and excluded from the calculation. Variable N shows the number of seasons calculated among 1-36 in a year.

$NDVI_{std}$ is used as an index that shows the disturbance of vegetation, because it shows the level of biomass increase and decrease every year. Standard deviation was sure to grow greatly in the region where the influence of a forest fire and the climate had been greatly received because the change of NDVI every year was large. Then, the standard deviation of ΣNDVI during year for an analytical period was requested. This parameter has already been used by Kondoh (2004). $NDVI_{std}$ was calculated by the following formula.

$$\mathrm{NDVI}_{\mathrm{std}} = \sqrt{V_x} \qquad V_x = \frac{1}{19}\sum_{i=1982}^{2000}(x_i - \bar{x})^2 \qquad \bar{x} = \frac{1}{19}\sum_{i=1982}^{2000} x_i$$

Variable x_i shows value of ΣNDVI from 1982 to 2000. Vx is variance.

For instance, both ΣNDVI and $NDVI_{std}$ change throughout the year in regions where floods and forest fire occur frequently and in regions where a big difference in the growth of vegetation by the timing of snow melting in each year.

The TRJ is an index that shows the direction of the land cover change. It is clarified that TRJ is different according to vegetation by Nemani and Running (1997). For instance, the value of TRJ shows positive when there is a tendency to the land cover change from the forest to the bare ground. And the inclination of the TRJ grows when the land cover changes from meadow to bare ground and the inclination of the TRJ declines when the land cover changes into forest. TRJ is obtained from the scatter chart of Ts and NDVI. NDVI is shown on the horizontal axis and Ts on the vertical axis. The value of TRJ is requested by calculating the inclination of the recurrence straight line after NDVI and the Ts data of 36 seasons are plotted. Ts was calculated by the following formula.

$$Ts = Ch.4 + 3.3 \times (Ch.4 - Ch.5)$$

With two channels *(Ch4, Ch5)* of the heat infrared rays, the split window method of Price (1984) was used to calculate the surface temperature[14)] . Therefore, the influence of the atmosphere is almost corrected. Ts is lower than -100℃ are judged as an error pixel and substitute error number zero.

TRJ was calculated by the following formula.

$$TRJ = \frac{\sum_{i=1}^{N}(a_i - \bar{a})(b_i - \bar{b})}{\sum_{i=1}^{N}(a_i - \bar{a})^2} \qquad \bar{a} = \frac{1}{N}\sum_{i=1}^{N} a_i \qquad \bar{b} = \frac{1}{N}\sum_{i=1}^{N} b_i$$

bi shows a *Ts* value of a season. Variable *N* shows the number of seasons calculated among 1-36 in a year. If NDVI is lower than 0.1 and Ts is lower than -100℃, the pixels are judged as error and excluded from the calculation.

Land-cover change can be calculated by applying a straight line to the tracks for every year, and analyzing the change in inclination of the straight line over 19 years. Trend of each parameter (TRJ, ΣNDVI, $NDVI_{max}$) were calculated by the following formula.

$$Trend = \frac{\sum_{j=1982}^{2000}(c_j - \bar{c})(d_j - \bar{d})}{\sum_{j=1982}^{2000}(c_j - \bar{c})^2} \qquad \bar{c} = \frac{1}{19}\sum_{j=1982}^{2000}(j - 1982) \qquad \bar{d} = \frac{1}{19}\sum_{j=1982}^{2000} d_j$$

Variable j means a value of year and *di* is substituted each parameter (TRJ, Σ NDVI, $NDVI_{max}$).

Moreover, the validity of the PAL data analysis results was verified by above-mentioned statistical material analysis and the regional field investigation; thus the areas in which the influence of artificial land alteration was greatest were determined.

V. Results and consideration

It is important for thinking about the land cover change to catch the climatic change of the Amur river basin in recent years. Because vegetation has received both the climate change and the man activity influences.

Therefore, the climatic change of the Amur river basin were first described.

1. CRU TS2.0 analysis

Figure 8 shows the secular variation in mean temperature at each month from 1982-2000 and figure 9 shows secular variation in annual mean temperature from 1961-1990 and 1982-2000.

First of all, when the secular variation of the annual mean temperature is seen, it is understood that+ 0.05℃/year rises overall from 1961-1990 (figure 9). From 1982-2000, the temperature rises in +0.07℃/year especially in the direction of the southwest of the Amur river basin. Therefore, it tends to Global warming though there is a regional difference in the Amur river basin.

However, any month is not clement on average but bias exists by the month. The mean temperature in February rises greatly by the whole area of the Amur river basin. Moreover, the mean temperature rise in the Amur river north is remarkable in October. On the other hand, the mean temperature in November and December decreases greatly in these regions.

The rise of the temperature at the early spring has the possibility of bringing the time of snow melting forward. It leads to the extension at the growth period in specific vegetation.

Figure 10 shows the secular variation in monthly precipitation at each month from 1982-2000 and figure 11 shows secular variation in yearly precipitation from 1961-1990 and 1982-2000.

First of all, when the secular variation in yearly precipitation is seen, year precipitation especially increases +7mm/year in the east part of Khabarovsk from 1961-1990 (Figure 11). On the other hand, Year precipitation has greatly decreased -10mm/year from 1982-2000 in the region. Year precipitation increases +7mm/year in the Amur river north. When analyzing the precipitation of every month, is understood that the precipitation change is large in the Amur river north in August (Figure 10).

But the change in precipitation is seen in the northern part of Amur river basin, the temperature is a restraining factor of the vegetation growth in the Northern Amur river basin especially[16]. Therefore, it is not easy to think that the influence of vegetation in this area on growth by a precipitation increase in summer is large. In a word, it is necessary to consider the temperature change in this region.

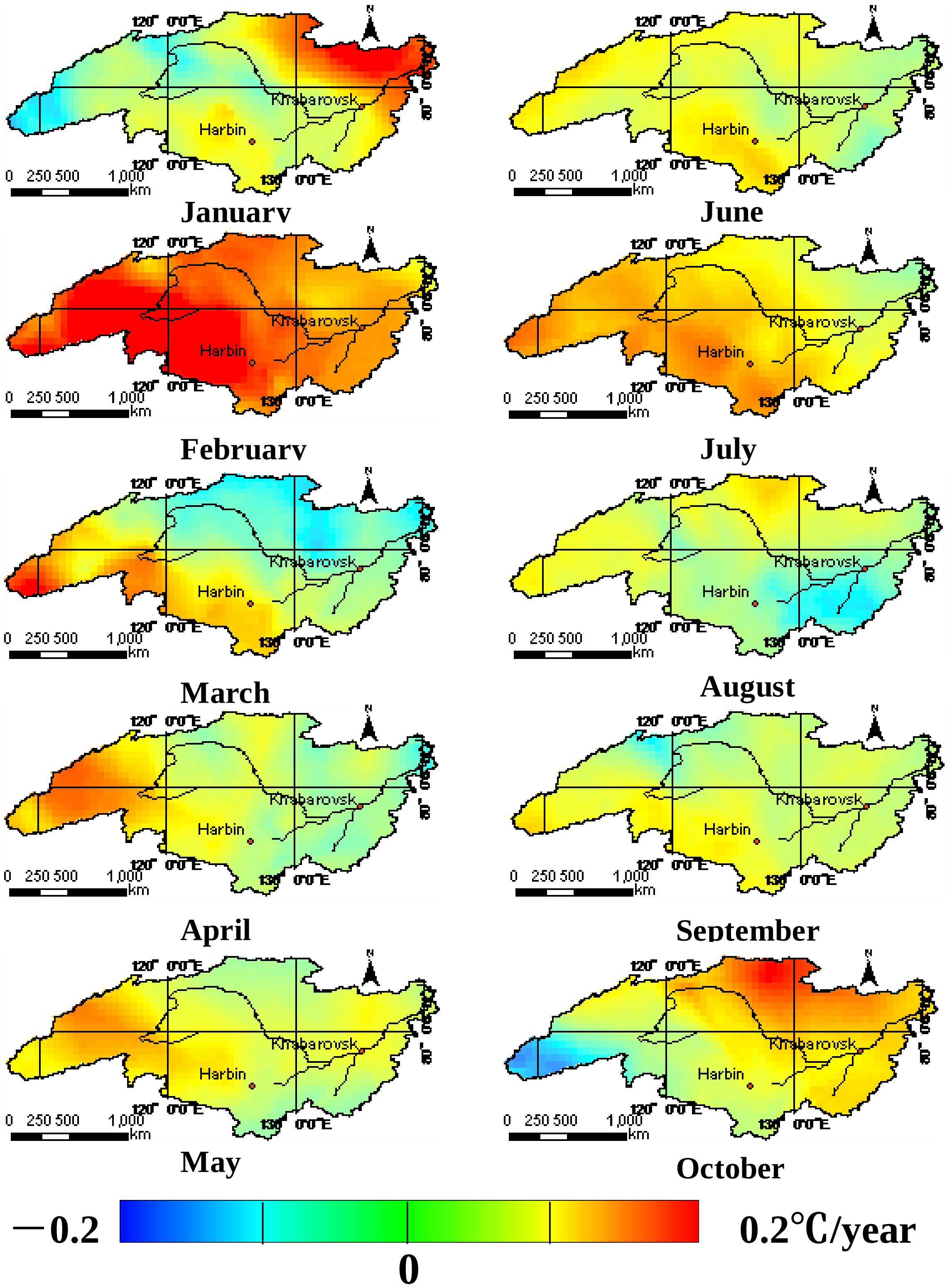

Figure 8. Secular variation in mean temperature at each month from 1982-2000 (January—October)

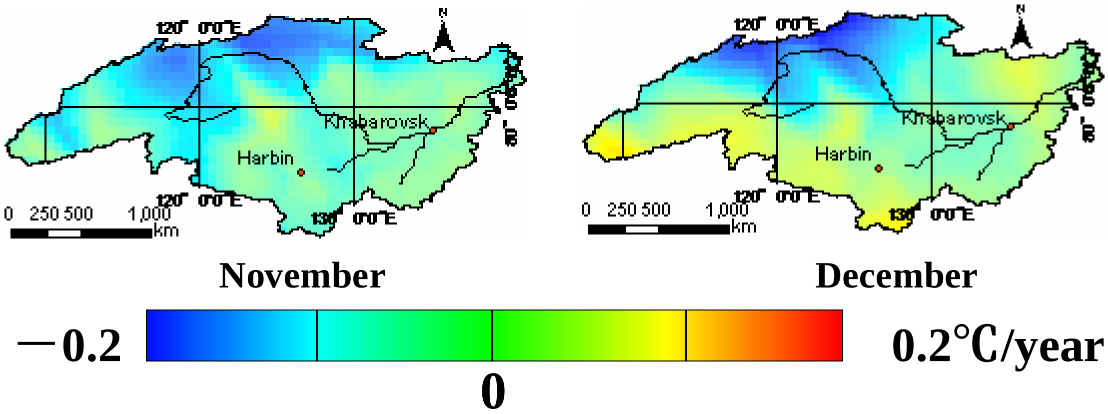

Figure 8. Secular variation in mean temperature at each month from 1982-2000 (November—December)

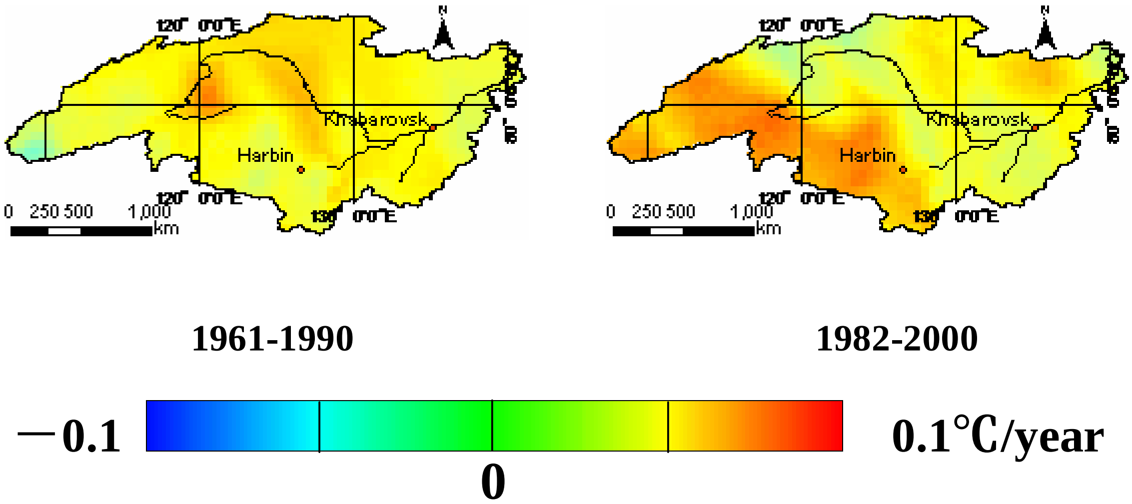

Figure 9. Secular variation in annual mean temperature from 1961-1990 and 1982-2000

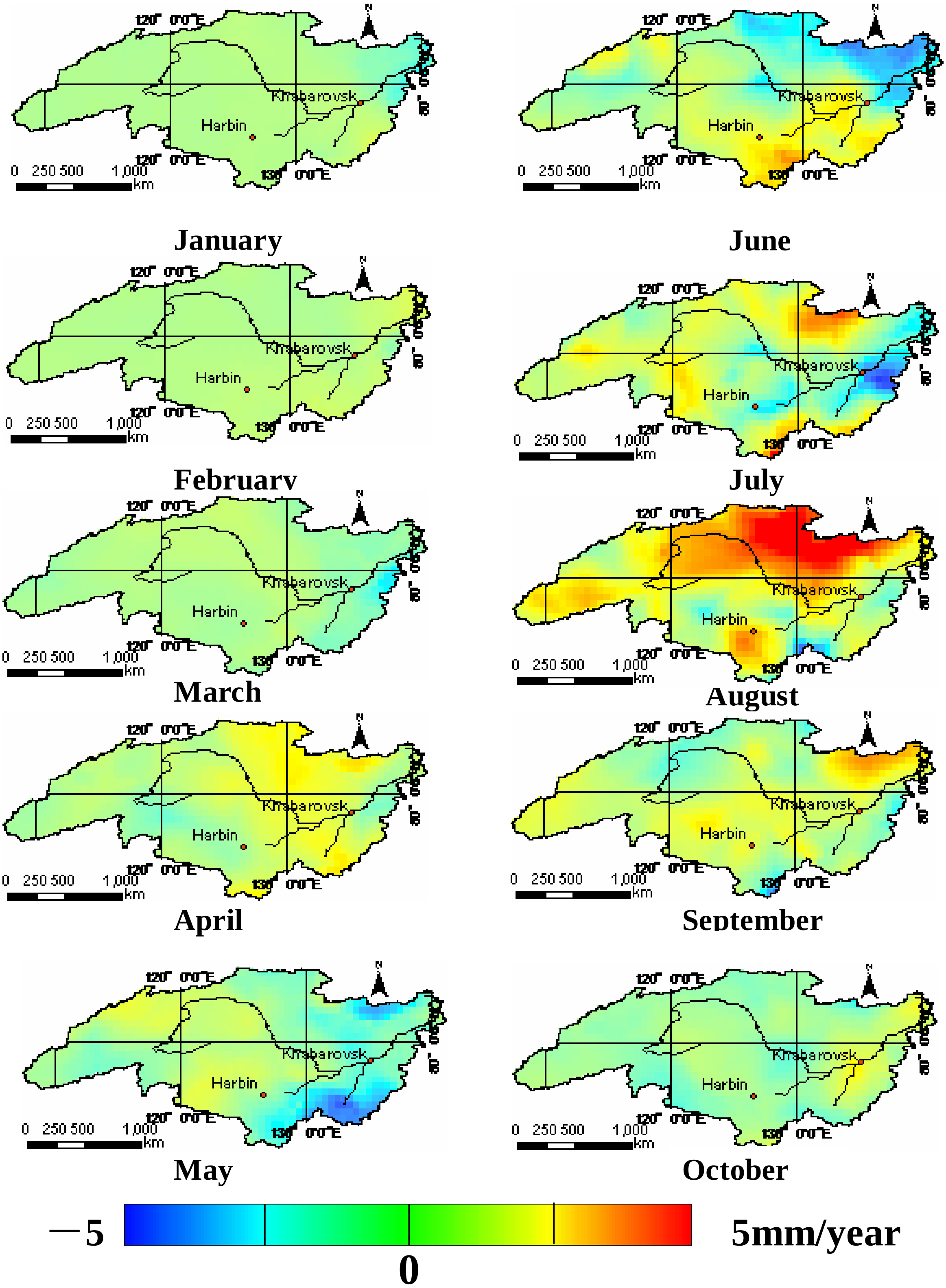

Figure 10. Secular variation in monthly precipitation

from 1982-2000 (January－October)

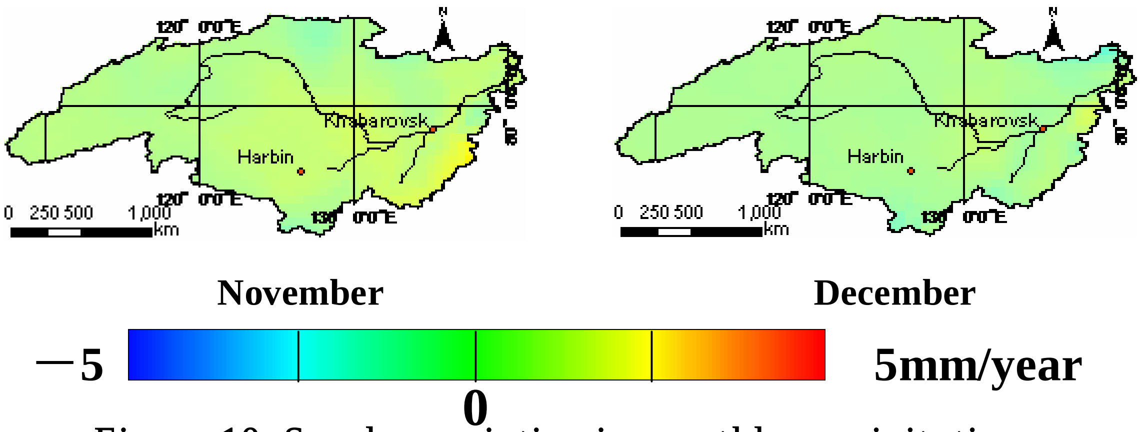

Figure 10. Secular variation in monthly precipitation from 1982-2000 (November—December)

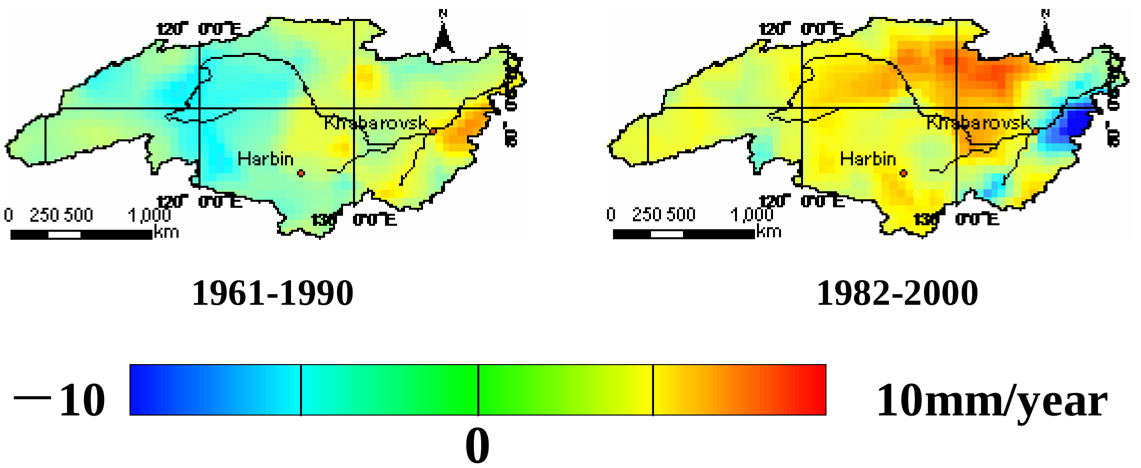

Figure 11. Secular variation in yearly precipitation

from 1961-1990 and 1982-2000

2. Analysis of secular variation in land cover from 1982 to 2000

Figure 12 shows the secular variation analysis of NDVI in the beginning of February between 1982 and 2000. As shown in the Figure 12, the NDVI value has hardly changed overall and the NDVI value has fallen below 0.1. This is because the Amur river basin is covered with the snowfall in winter. But there is an area where NDVI exceeds 0.1 in the east part of the Amur river basin though it is winter. It is because vegetation that is not the deciduous forest in this region either is distributed. Compared with the altitude, the area was distributed in a low mountainous district 500 to 1300 m asl.

Figure 13 shows the secular variation analysis of NDVI in the beginning of August between 1982 and 2000. As shown in the Figure 13, the NDVI value indicates large change depending on years. The value of NDVI is large in the entire Amur river basin in 1989, 1994, and 1995 especially. However, 1985 and 1993 have become small. It is thought that NDVI reflects meteorological conditions of every year, and catches the activity of vegetation certainly because this is a change on the large scale. When NDVI changes in the plains part and the mountainous district are compared, the change of the mountainous district is relatively larger. And the region where NDVI extremely becomes small by the year like the northern part of the Amur river of 1983 and 1996 is also seen. In meteorological analyses, the Amur river basin tends to Global warming. However, when Figure 13 is seen, NDVI understands the change by the year is large. Therefore, the influence of Global warming is high a secondary possibility.

There is a big difference in NDVI in winter and summer. Moreover, the difference of NDVI in each year is plain for summer. However, it is difficult to find the land cover change from these figures. Then, it is necessary to analyze the secular variation.

The NDVI value falls below the threshold in winter because the Amur River basin is covered with snow. Therefore, the secular variation in each parameter represents the NDVI changes from early spring to autumn. Figures 14 to 17 show the changes in each NDVI index in the Amur River basin over the 19-year period (1982–2000). From among these results I selected and interpreted five regions in which the changes in each parameter were clear.

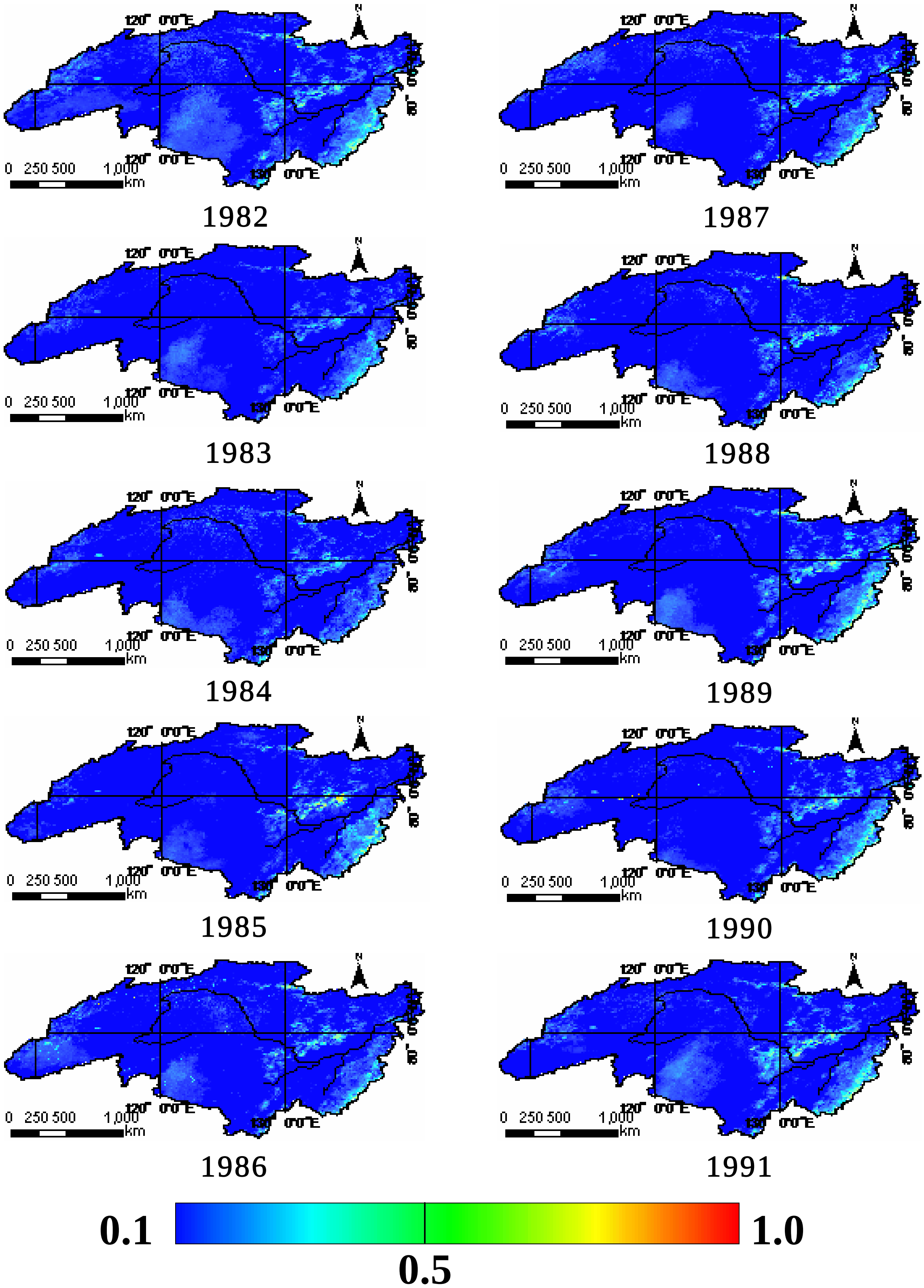

Figure 12. NDVI value in the beginning of February from 1982-2000 (1982—1991)

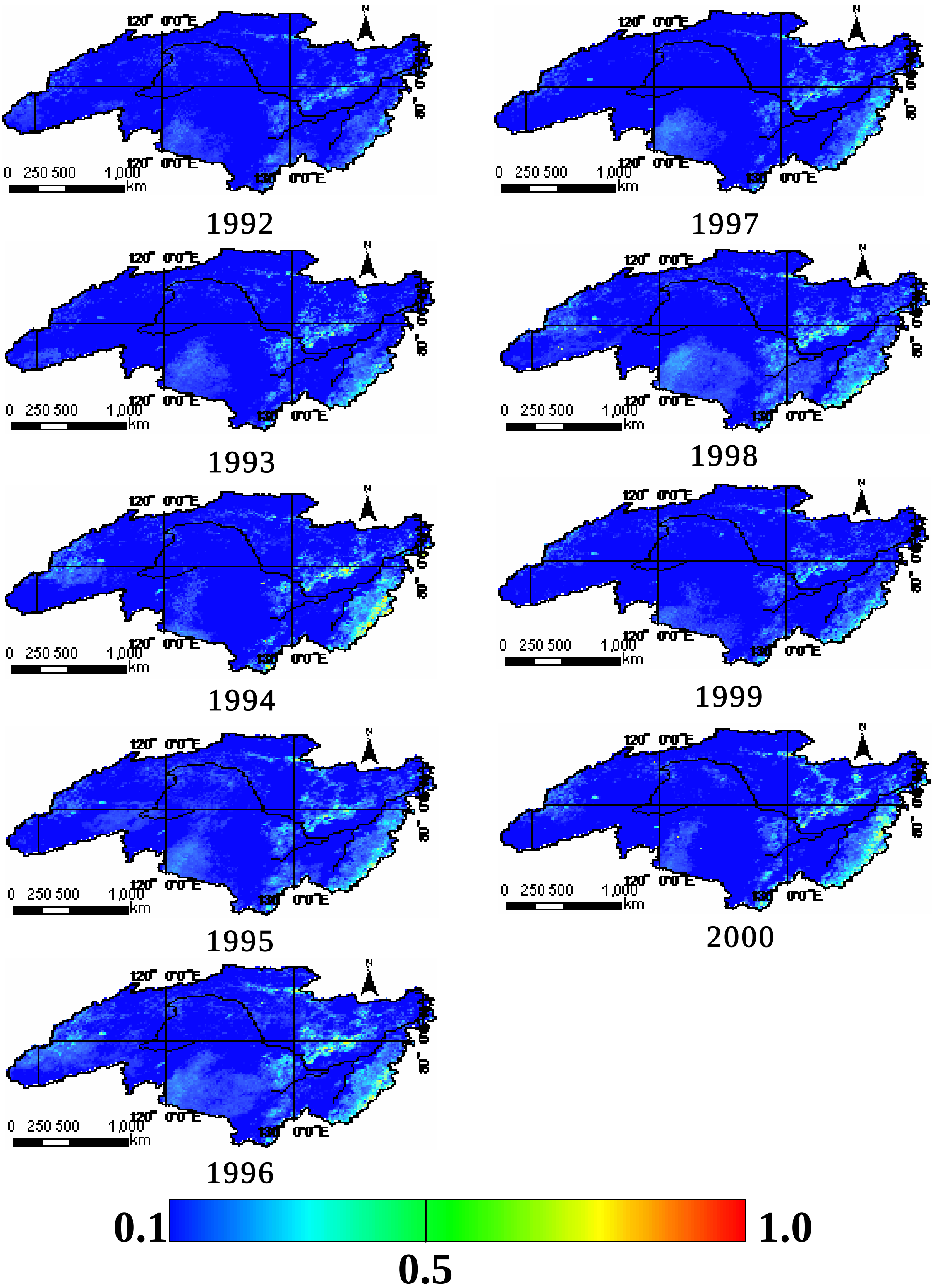

Figure12. NDVI value in the beginning of February from 1982-2000 (1992—2000)

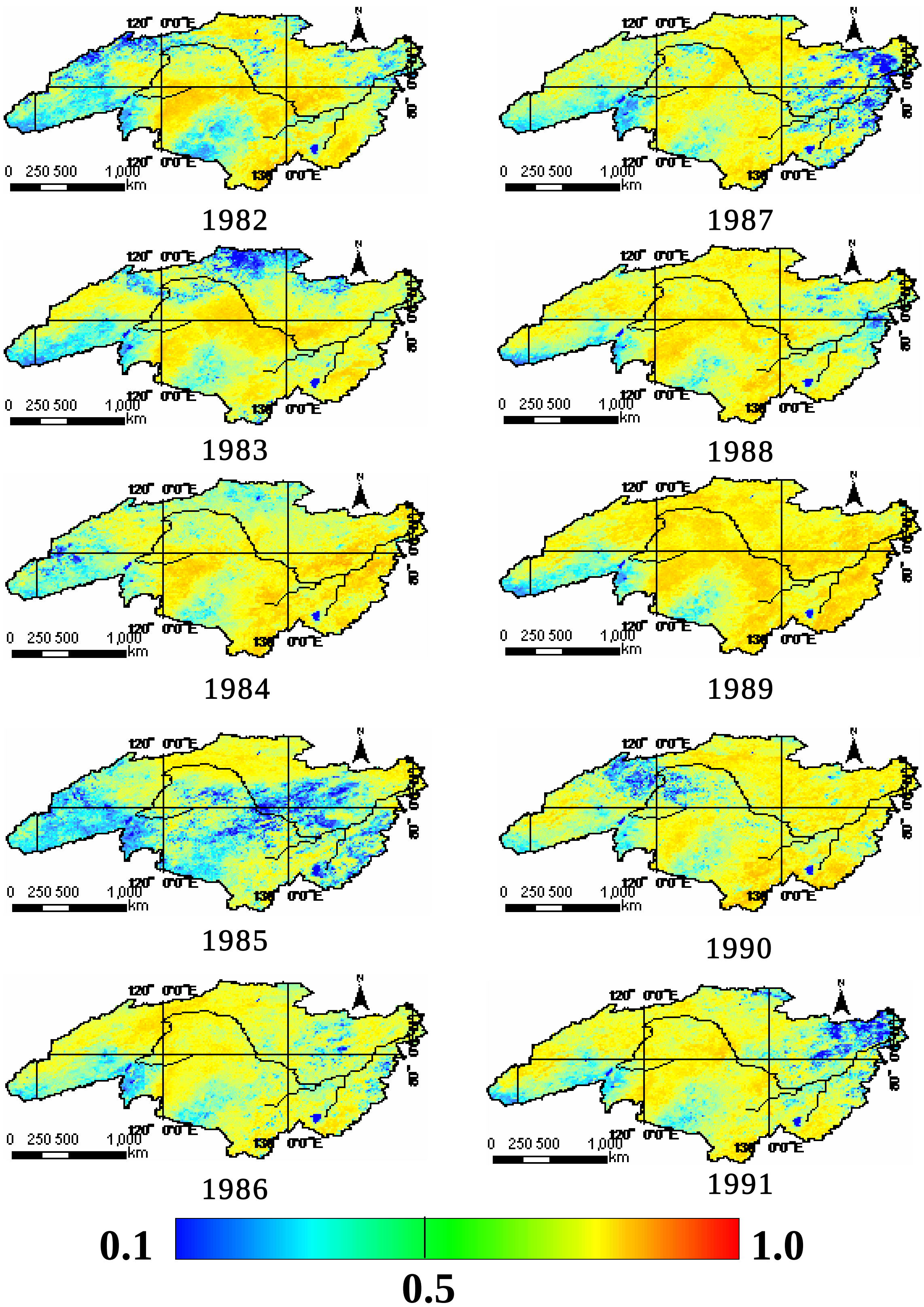

Figure13. NDVI value in the beginning of August from 1982-2000 (1982—1991)

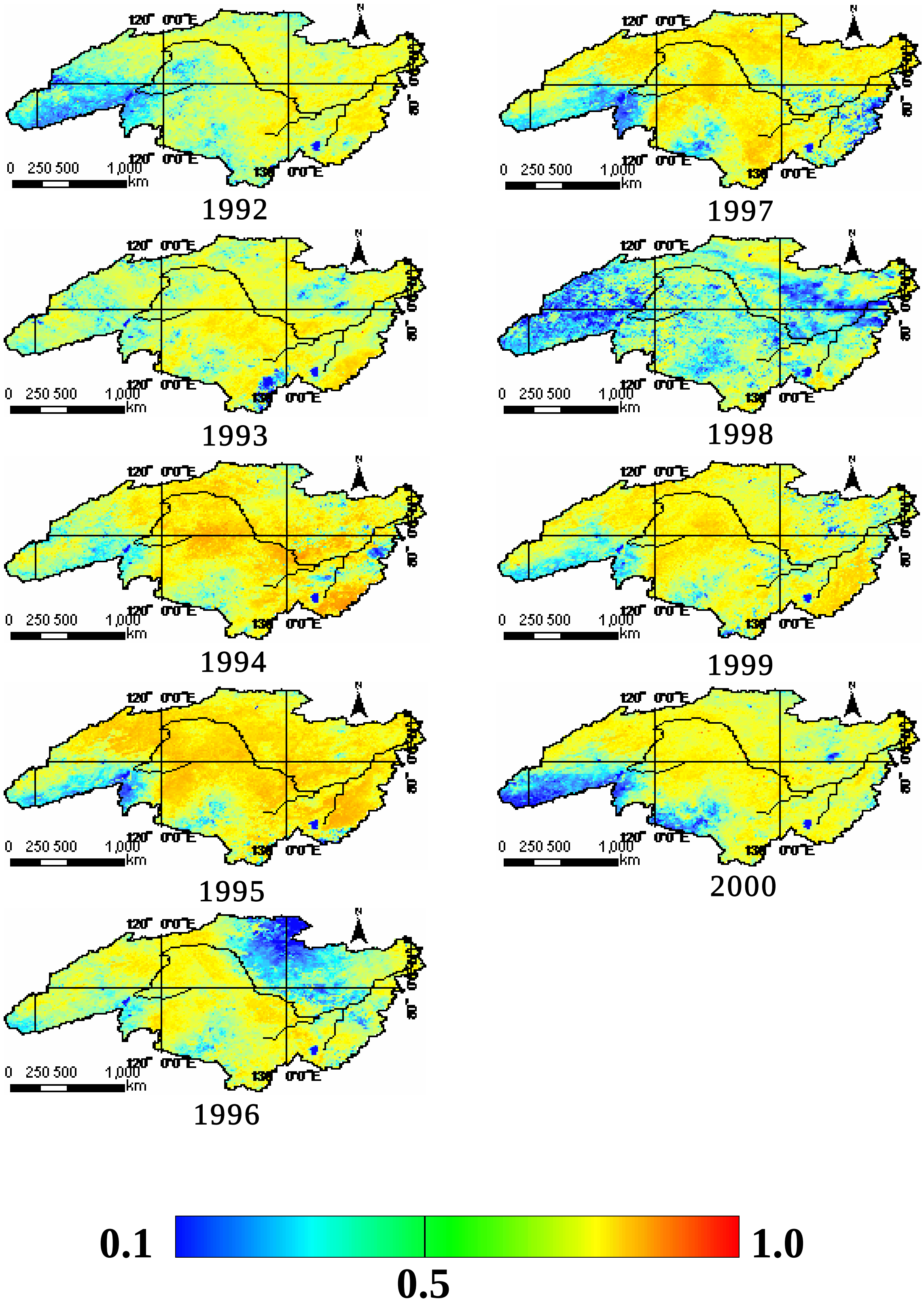

Figure13. NDVI value in the beginning of August from 1982-2000 (1991—2000)

1-a. Area 1

Area 1 is located between lat 52.75°–54.85°N and long 116.75°–130.35°E and is covered by extensive coniferous forest. The vegetation data set that Olson et al. had made was referred to for the vegetation zone[17]. Figure 15 shows that the value of ΣNDVI increased over this area. The area of ΣNDVI = 0.05 or more extended both east and west and was distributed in a low mountainous district 500 to 800 m asl. $NDVI_{std}$ was also high (1.5 or more) (Figure 16) in the area where ΣNDVI is high. No remarkable change in $NDVI_{max}$ (Figure 14) or TRJ (Figure 17) was seen across the region.

In 1997 Myneni found increased vegetation activity and discussed the relationship of this activity to global warming in northern Eurasia, Alaska, and the Canadian northwest (lat 45°00–70°00N) during the period 1982–1990 [7]. Moreover, the temperature rose by 4 °C in winter in these three regions during 1961–1990 [18]. In the analysis of the CRU data of this study, it was confirmed that the mean temperature in February had risen between 1982 and 2000. Therefore, this temperature change appears to have been reflected in an increase in ΣNDVI in that the vegetation growth period was extended: the snow melted in early spring because the temperature rose early in winter. Moreover, the value of $NDVI_{std}$ increased because the difference in ΣNDVI within each year was large and it is a vegetation zone where the influence of the climate is received easily; Area 1 can thus be interpreted as a region influenced readily by both yearly changes in meteorological conditions and global climate change.

1-b. Area 2

Area 2 is located at lat 43.65°–50.15°N and long 134.65°–140.75°E. In this region coniferous forests extend from 500–1300 m asl. An area where $NDVI_{std}$ was greater than 1.5 (Figure 16) and ΣNDVI was 0.05 (Figure 15) was distributed from southwest to northeast along the basin's boundary. No marked change was seen in $NDVI_{max}$ or TRJ (Figures 14, 17). However, an area of ΣNDVI = –0.21 (decreased biomass) extended from Khabarovsk to about 250 km eastward. Large-scale forest fires occurred in Khabarovsk Territory in 1976, 1998–1999, and 2001, and the Far Eastern taiga covering 25,000 km^2 received damage in 1998 [19]. I consider that this decrease in ΣNDVI in Area 2, and thus the decrease in biomass, resulted from the frequent forest fires. Or, NDVI falls below the threshold for a large amount of smoke at a forest fire and there is a possibility that NDVI is not added to ΣNDVI.

1-c. Area 3

Area 3 is located at lat 47.00°–50.00°N, long 114.50°–118.00°. In this region the plateaus and hills extend to 550–900 m asl. The area has a steppe climate, and the main region is covered by meadow vegetation. The whole area had TRJ = 3 (Figure 17), but ΣNDVI, $NDVI_{max}$, and $NDVI_{std}$ (Figures 14, 15, 16) showed no marked changes.

Therefore, the increase in TRJ must be derived from an increase in Ts. Generally, with meadow vegetation such as that in Area 3, there is a period of bare ground between snow melting and foliation. Consideration of ΣNDVI, $NDVI_{max}$, $NDVI_{std}$, and the vegetation of Area 3 leads to the interpretation that the period of bare ground increased over the 19 years, and the Ts rose because snow melt occurred increasingly early; as a result, the TRJ increased.

Moreover, when supplementing for the NDVI index, an increase in the bare ground period is not simply related to an increase in the biomass in the meadow vegetation of Mongolia. Because it receives a complex influence according to the temperature, precipitation and soil water content[20]. Kondoh *et al.* (2002) divided the vegetation zone in the world into the vegetation zone of the water dependence and the energy dependence[21], Area 3 is located in the transition belt of both. When the influence of the climate change and the man activity expected in the 21st century is foreseen, the boundary of the ecology zone is thought to be the weakest region. Therefore, it is scheduled that it keeps monitoring in the future and a detailed research is done about an increase of TRJ in this area.

1-d. Area 4

Area 4 is located at lat 46.55°–47.85°N, long 129.55°–134.05°E. This region is known as the Sanjiang Plain, and here the floodplain is distributed to about 50–70 m asl. In figure 14, the value of $NDVI_{max}$ is growing in the low ground part where agriculture is being actively done recently. North and south part of the Songhua River, the $NDVI_{max}$ = 0.008 (Figure 14) and the TRJ was about –3.0 (Figure 17). In particular, the changes in these parameters on the floodplain between the Songhua River and the Amur River are plain. When biomass increases and the conditions for vegetation growth improve, transpiration becomes active and Ts decreases. Moreover, the heat budget at ground level is changed by water transmission via irrigation and Ts decreases [12)]. TRJ decreased by these factors. Therefore, the secular variation in each parameter in Area 4 can be interpreted as showing land-cover change through the development of agricultural activity.

From viewpoint of biological diversity, the wetlands in this plain are important natural environment. Further research is requested about what influence the reclamation of the wetland gives natural environment especially, in this area.

1-e. Area 5

Area 5 is located at lat 44.75°–48.75°N and long 121.85°–128.05°E and is called the Songnen Plain. An increase in $NDVI_{max}$ (Figure 14) was clear on the floodplain and on the hills, which are at an altitude of about 130–280 m. The $NDVI_{max}$ was 0.005 in the hill zone to the north of the city of Harbin. The hill zone to the west or southwest of the city of Quiqihar had a larger $NDVI_{max}$ (0 .006). ΣNDVI and TRJ (Figures 15, 17) also showed obvious changes in the floodplain and hill zones: TRJ was below –1 and ΣNDVI equaled 0.1.

In Area 5, an area that extends for 200 km north of the city of Harbin and has seen a marked expansion in the area under rice cultivation since the 1980s [4)], the ΣNDVI was 0.08 and the $NDVI_{max}$ was 0.005 (Figures 14, 15). The trends in each parameter were similar to those in Area 4 and can be interpreted as indicative of land-cover change in response to the development of agricultural activity. ΣNDVI increased in the low mountainous districts (especially those higher than 200 m asl), suggesting that increases in afforestation, as well as in agricultural activity, increased the ΣNDVI[4)].

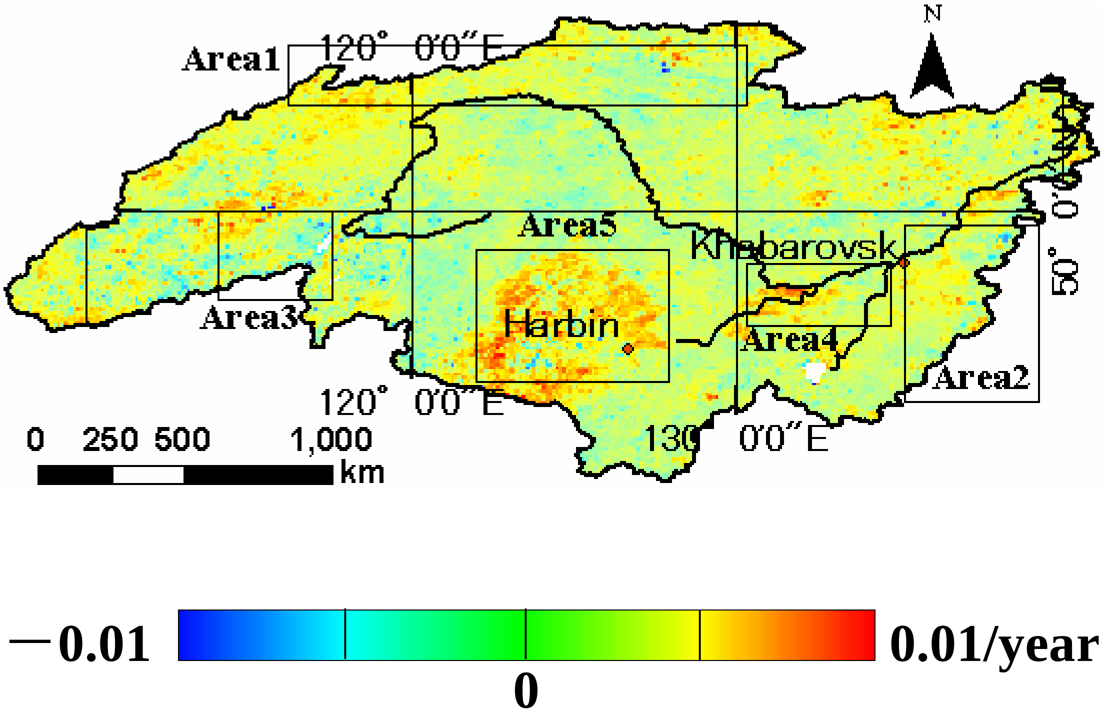

Figure 14. $NDVI_{max}$ (secular variation 1982–2000)

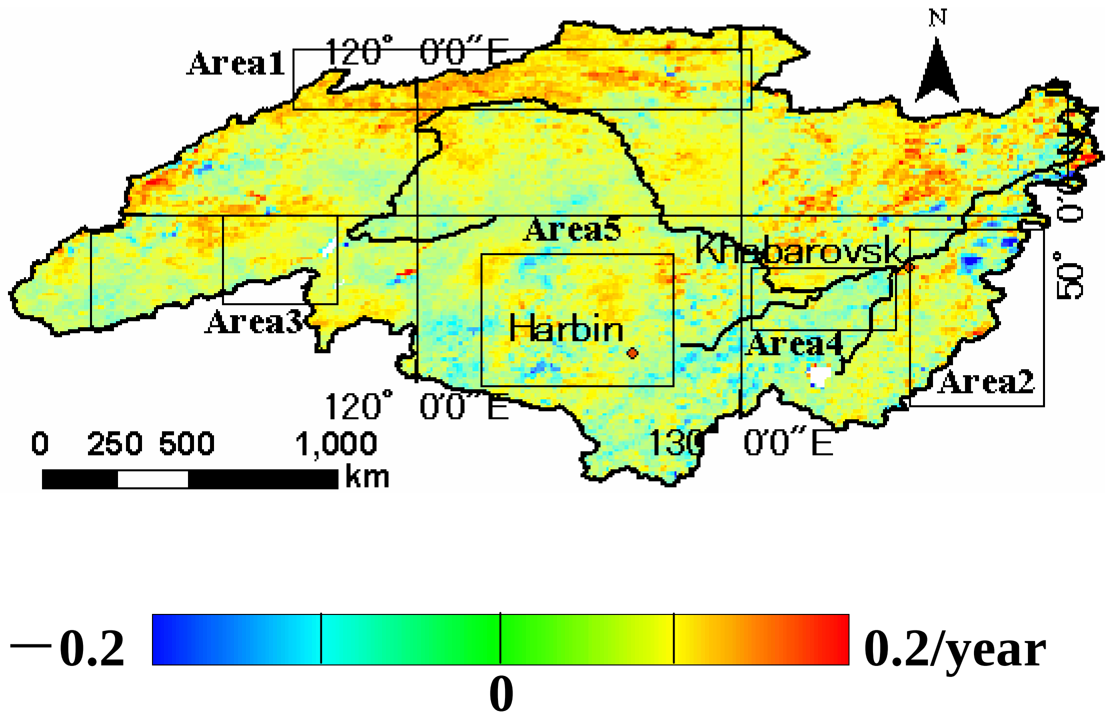

Figure 15. ΣNDVI (secular variation 1982–2000)

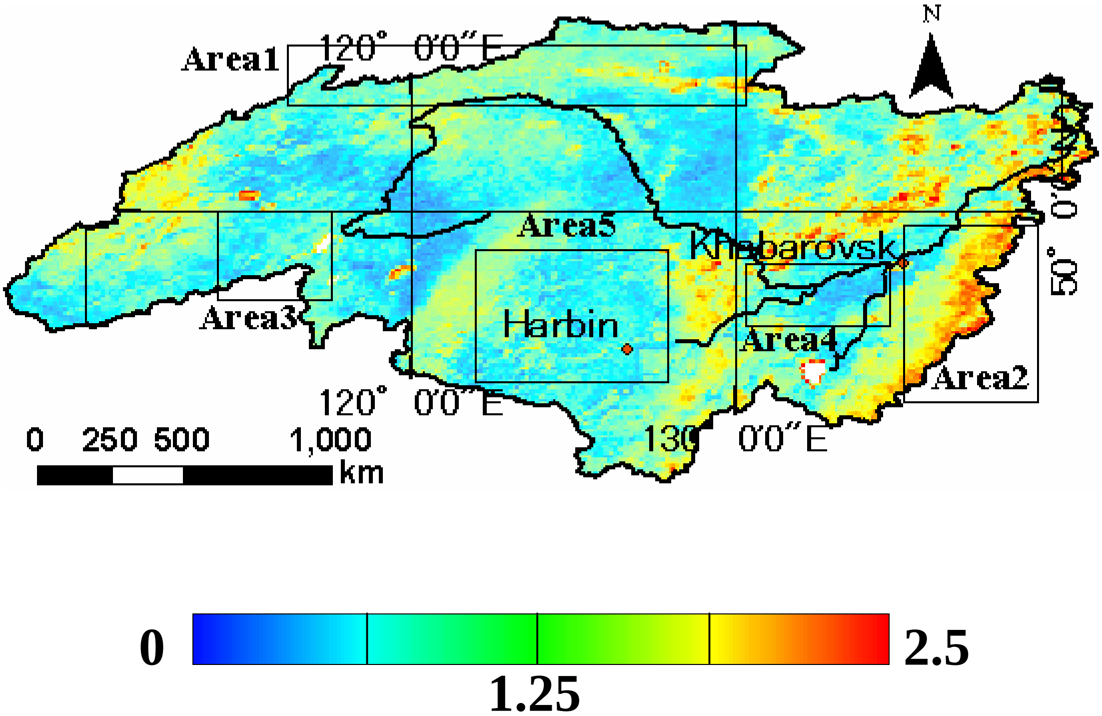

Figure 16. NDVI$_{std}$ (secular variation 1982–2000)

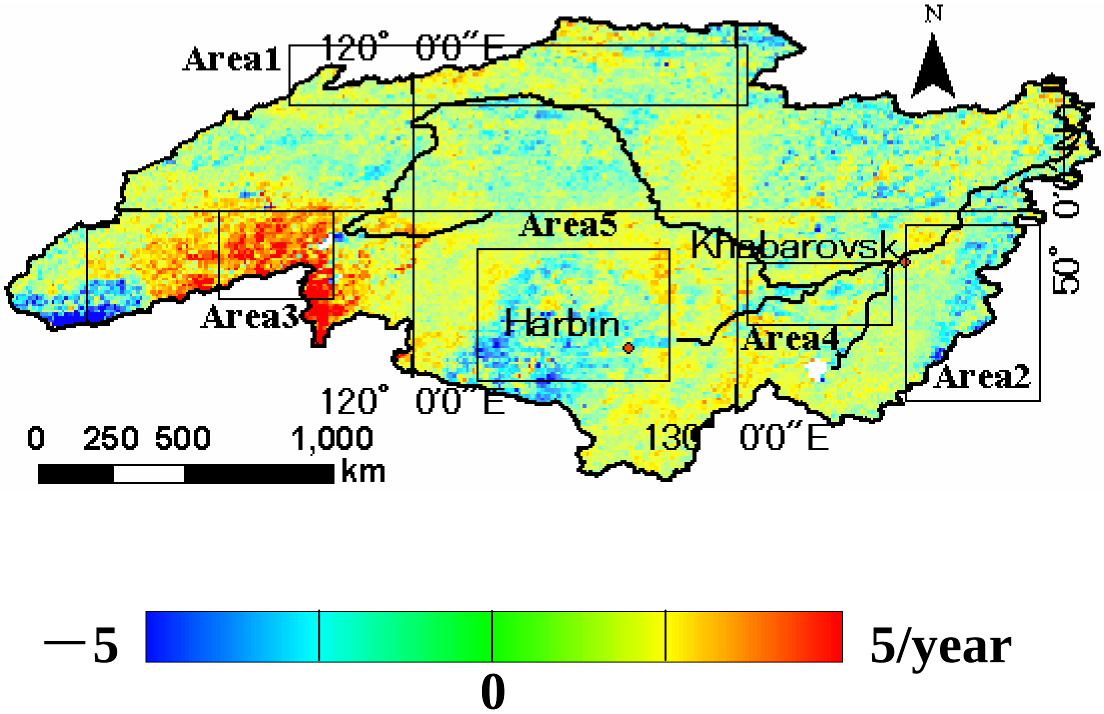

Figure 17. TRJ (secular variation 1982–2000)

3. Verification of validity of PAL data analysis

The validity of PAL data analysis was verified by analyzing agricultural statistics from Heilongjiang Province. Statistics for Areas 4 and 5 were used, because I considered that the influence of artificial land alteration was the greatest in these two areas out of the whole Amur River basin. These regions are important food production regions of Heilongjiang Province.

The area of Heilongjiang Province under irrigation expanded rapidly by 300% or more (from 670,500 to 2,032,000 ha) in the 21 years from 1980 through 2000 (Figure 18). The area sown to commercial crops (Rice, wheat, corn and soybean) and the production of rice increased greatly in the 23 years from 1978 through 2000 (750%—214,100 to 1,606,000 ha—in the case of planted area and 1460%—715,000 to 10,422,000 t—in the case of rice harvest (Figures 19, 20).

Moreover, the increase of corn production is remarkable in the first half of the 90's. And in the rice farming, both area and production increase as a rapid increase of the irrigation area since the latter half of the 90's.

Figure 21 is that shows the transition of all cultivated acreages, the rice farming areas, and the areas of plowing a field in Heilongjiang province from 1978 to 2000. As shown in the Figure 21, all cultivated acreages and the rice farming areas will keep increasing in about 20 years, On the other hand, the decreasing tendency since the latter half of the 1980's is indicated in the area of plowing a field. It is thought that an increase in the irrigation area is due to an increase in the rice farming area in comparison to the figure 18.

In our September 2005 field investigation, I confirmed that floodplains were being used for rice fields, hillside terraces for soybean fields, and hills for cornfields. Only parts of the wetlands remained (Figure 5, 6).

Therefore, in Area4 and 5, the irrigation maintenance is done to the upland farming (Wheat, corn and soybean) at the beginning of the 1990's, and the irrigation area has increased. As a result, it is thought that production increased around corn fields. On the other hand, an increase in the irrigation area in the latter half of the 1990's is thought to be rice field development by the wetland reclamation because of the increase of rice production and sown area in this period.

In this area, there is a part where the precipitation in August exists in the increasing tendency. However, the signal of the land cover change is confirmed by $NDVI_{max}$ and TRJ also in the point where the change tendency to precipitation is small in this area.

The land cover change by the development of an agricultural activity was shown by analyzing PAL dataset in these regions. It is thought that this analysis caught the change in an agricultural form like the above-mentioned.

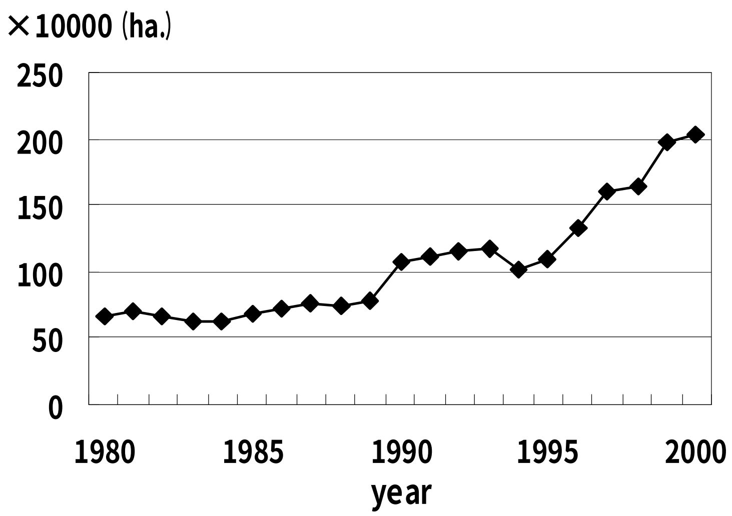

Figure 18. Transition of area under irrigation in Heilongjiang Province

Table1. Transition of area under irrigation in Heilongjiang Province（Table）

Unit: 10000ha.

Year	Irrigation area	Year	Irrigation area
1980	67.05	1991	111.78
1981	69.83	1992	115.7
1982	67.36	1993	116.36
1983	63.1	1994	101.54
1984	62.36	1995	109.5
1985	67.95	1996	133.5
1986	71.97	1997	160.7
1987	76.63	1998	164.8
1988	73.96	1999	196.6
1989	77.75	2000	203.2
1990	107.87		

China Map publishers（2004）

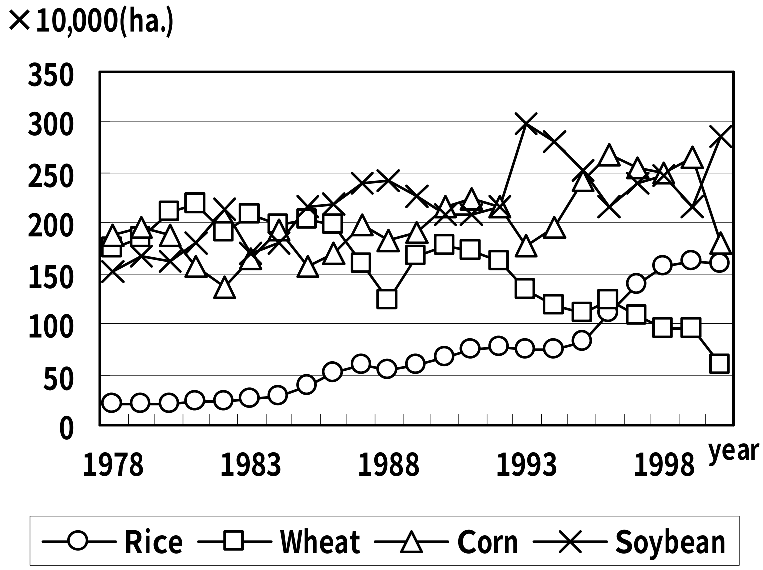

Figure 19. Transition of area sown to commercial crops in Heilongjiang Province

Table2. Transition of area sown to commercial crops in Heilongjiang Province (Table)

Unit: 10000ha.

Year	Rice	Wheat	Corn	Soybean
1978	21.41	174.72	189.04	152.49
1979	20.63	185.93	196.08	166.51
1980	21.04	210.52	188.4	163.01
1981	22.41	219.03	157.7	179.97
1982	23.92	190.43	136.34	213.55
1983	24.55	209.63	164.16	169.25
1984	27.75	198.02	192.01	179.54
1985	38.97	203.79	157.66	216.74
1986	50.69	196.91	168.9	219.67
1987	58.06	158.69	197.55	239.95
1988	55.29	123.87	182.75	242.89
1989	60.41	168.18	190.35	226.38
1990	67.35	178.11	216.85	207.87
1991	74.69	173.68	223.01	209.42
1992	77.84	161.46	216.59	216.02
1993	73.55	133.65	177.68	297.92
1994	74.82	119.47	196.41	279.57
1995	83.5	111.6	241.1	251.3
1996	110.9	123.7	266.6	216.1
1997	139.7	107.4	254.5	239.4
1998	156.3	95.9	248.6	246
1999	161.5	95.3	265.2	215.3
2000	160.6	59	180.1	286.8

China Map publishers（2004）

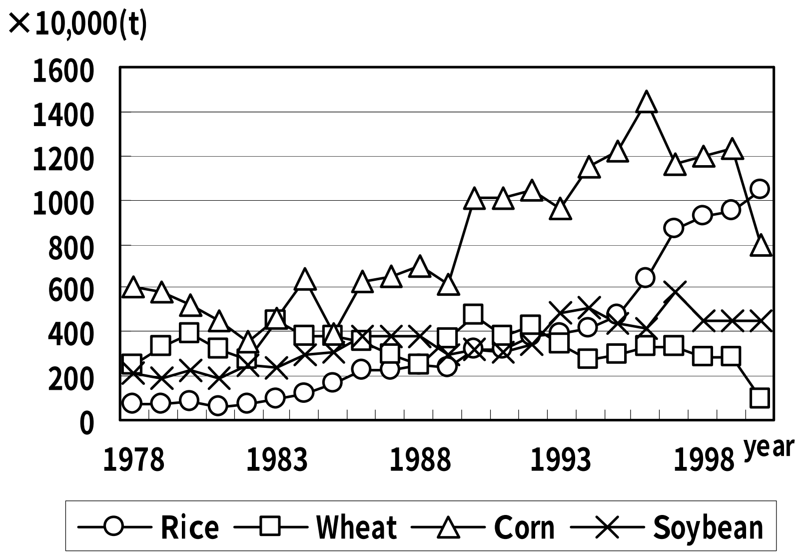

Figure 20. Transition in production of commercial crops in Heilongjiang Province

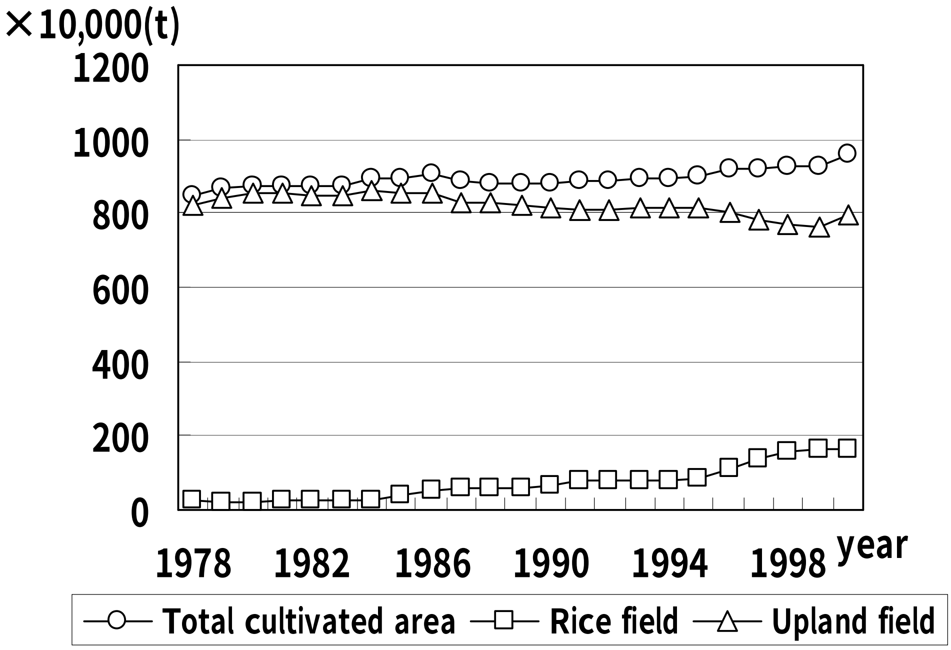

Figure 21. Transition of total cultivated area, rice field and upland field in Heilongjiang Province

Table 3. Transition in production of commercial crops

in Heilongjiang Province (Table)

Unit: 10000t

Year	Rice	Wheat	Corn	Soybean
1978	71.5	254.5	602	208
1979	71.7	333.2	581	185.5
1980	79.6	394.6	520	220.5
1981	55.7	314.1	455	188.3
1982	70.9	268.2	352.6	245.5
1983	91.5	451	463.5	238.5
1984	124	382.5	642	290.5
1985	162.9	376.8	386.8	313.7
1986	220.8	355.9	632	378
1987	225.7	299.8	646.1	383.5
1988	243.5	250.4	700.6	384.4
1989	231.7	367.3	615.2	291.8
1990	314.4	474.8	1008.3	325.8
1991	316.2	381.1	1007.5	309.8
1992	376.6	424.8	1042.8	349.1
1993	388.3	340	956.6	491.5
1994	410.4	275.3	1146.4	513.6
1995	469.9	293.4	1219.1	438.8
1996	636.6	329.5	1445	413.5
1997	860.9	328.4	1165.9	576.2
1998	925.8	285.2	1199.7	444.6
1999	944.3	284.2	1228.4	446.6
2000	1042.2	95.8	790.8	450.1

China Map publishers（2004)

Table 4. Transition of total cultivated area, rice field

and upland field in Heilongjiang Province

Unit: 10000ha.

Year	Total cultivated area	Rice field	Upland field
1978	845.8	22.9	822.9
1979	866.3	22	844.3
1980	872.6	21.5	851.1
1981	875.5	22.9	852.6
1982	871.9	24.5	847.4
1983	875.1	25.5	849.6
1984	890.9	28.7	862.2
1985	893.1	39.4	853.7
1986	905	51.1	853.9
1987	885.9	57.8	828.1
1988	883.4	56.4	827
1989	882.6	60.9	821.7
1990	883.1	68.1	815
1991	884.7	75.6	809.1
1992	890	79.1	810.9
1993	890.8	78.1	812.7
1994	890.9	77	813.9
1995	899.5	86.9	812.6
1996	917.5	114.1	803.4
1997	922.4	139.9	782.5
1998	924	156.3	767.7
1999	926	161.5	765.1
2000	961.7	164.7	797

China Map publishers (2004)

VI. Summary

I demonstrated the trends in land-cover change in the Amur Basin from 1982 to 2000 spatially by using four indices calculated from the NDVI. Moreover, I was able to explain the land-cover change in five selected areas by combining and interpreting these indices. As a result, the following of each area were clarified.

Area 1 and 2 can be interpreted as a region influenced readily by both yearly changes in meteorological conditions and global climate change. An increase of ΣNDVI and NDVIstd in this region was considered from the analysis of the meteorogical data set and the past research. It was able to be concluded that the change in the NDVI index was by the rise of the temperature in winter and snow melting of an early stage.

Land-cover change in the Amur River basin by the human factor is especially remarkable in the grain production region of Heilongjiang Province in China (Area4, 5). To validate the results of the PAL data analysis, I performed a statistical material analysis and field investigation for Areas 4 (Sanjiang Plain) and 5 (Songnen Plain). I confirmed that the secular variation in each parameter in these regions was associated with arable land development for irrigation and with land-cover changes from rice farming development.

The change in the NDVI index of Area 3 cannot be declared only by this research. Because it receives a complex influence according to the temperature, precipitation and soil water content in this area. When the influence of the climate change and the man activity expected in the 21st century is foreseen, the boundary of the ecology zone is thought to be the weakest region. Therefore, it is scheduled that it keeps monitoring in the future and a detailed research should be done in this area.

By this reserch, It was clarified that in which part of the Amur river basin the land cover change was remarkable. Especially, the conversion of the wetland to the farmland has the possibility of influencing the ecosystem of the Amur river basin. In the future, it is expected that a detailed research on spatial change in wetland area using satellite image of high resolution and on the change in the flux of the material to the Amur river according to the reclamation of wetland. Moreover, this thesis is a research that applies the technique of global analysis using PAL data by Kondoh 2004 to the local analysis for the first time. This local analysis will be expected to be applied to other regions in the future.

Acknowledgment

The author would like to express his sincere appreciation to assistant Prof. Shigeko Haruyama for her continuous supports and valuable suggestions to accomplish this work. He also expresses thanks to Prof. Akihiko Kondoh, Center for Environmental Remote Sensing, Chiba University for his helpful comments and discussions throughout the course of this work.

He is thankful to assistant Prof. Kotaro Yamagata, Joetsu University of Education and Dr. Dexuan Wang, Northeast Institute of Geography and Agricultural Ecology, Chinese Academy of Sciences for his help with obtaining the ground truth data. He is grateful to Ms. Mizue MUROOKA, Hokkaido Abashiri Fisheries Experiment Station for her valuable assistance and warm encouragement.

He is indebted to assistant Prof. Takayuki Shiraiwa, the Research Institute for Humanity and Nature (RIHN) for proceeding this work. Special thanks are extended to asistant Yasushi Agata for providing a helpful IT environment. He also thanks to Mr. Yuichi Ikeda, Mr. Taro Hamada and Mr. Nobuhide Suzuki for making a comfortable environment.

He expresses gratitude to Mr. Muraoka, Graduate school of Science and Technology, Chiba University for making some figures clear. All the member of Department of Natural Environmental Studies, Graduate School of Frontier Science, University of Tokyo and Kondoh laboratory of Center for Environmental Remote Sensing, Chiba University are appreciated.

References

1) Ganzey S.S. (2005): Transboundary Geo-Systems in the South of the Russian Far East and in Northeast China. Vladivostok, Dalnauk, 148-159.

2) Motoki Y. (2001): Agricultural land use change of north east China—view of role of rice production. LU/GEC (LandUse for Global Environmental Conservation) Project Report VII, CGER-REPORT, CGER-1048-2001, 83–98, [in Japanese]

3) Shiraiwa T. (2005): The Amur Okhotsk Project. Report on Amur-Okhotsk Project, No. 3, December 2005, Research Institute for Humanity and Nature, 1–2

4) Himiyama Y. (2001): Land use change in northeast China—GIS database and evaluation for sustainable development. LU/GEC LandUse for Global Environmental Conservation) Project Report VII, CGER-REPORT, CGER-1048-2001, 83–98, [in Japanese]

5) *China Map publishers （2004） :*Atlas of China. China Map Publishers, Beijing, China, [in Chinese]

6) Lin M., Hasegawa K. (2005): The problems on the Large-Scale management of rice production in Heilongjiang Province—A case study on G-Village in Fujin city—. Bulletin of Department of Agriculture, Mie University, 32, 61–78, [in Japanese]

7) Myneni R. B., Keeling C. D., Tucker C. J., Asrar G., Nemani R. R. (1997): Increased plant growth in the northern high latitudes from 1981 to 1991. Nature 386, 698–702

8) Sannier C. A. D., Taylor J. C., du Plessis W., Campbell K. (1998): Real-time vegetation monitoring with NOAA/ AVHRR in southern Africa for wildlife management and food security assessment. International Journal of Remote Sensing, 19(4), 621–639

9) Spanner M. A., Pierce L. L., Running S. W., Peterson D.L. (1990): Seasonal AVHRR data of temperature coniferous forests: relationship with leaf area index. Remote Sensing of Environment 33, 97–112

10) Box E. O., Holben B. N., Kalb, V. (1989): Accuracy of the AVHRR vegetation index as a predictor of biomass, primary productivity and net CO2 flux. Vegetatio 80, 71–89.

11) *China Statistics Publishers (2001)*: Statistics of Heilongjiang Province. China Statistics Publishers, Beijing, China

12) Akihiko K. (2004): Analysis of vegetation and land cover change using global remote sensing. Japan Society of Hydrology and Water Resources, 17(5), 459–467,

[in Japanese]
13) Nemani R., Running S. (1997): Land cover characterization using multitemporal red, near-IR and thermal-IR data from NOAA/AVHRR. Ecological Applications 7(1), 79–90.
14) Price C. J. (1984): Land surface temperature measurement from the split window channels of the NOAA 7 Advanced Very High resolution radiometer. Journal of Geophysical Research 89, 7231–7237.
15) Goward, S. N., Tucker, C. J., and Dye, D. G.(1985):North American vegetation patterns observed with the NOAA-7 advanced very high resolution radiometer. Vegetatio,64, 3-14
16) Ramakrishna R.Nemani,Charles D. Keeling, Hirofumi Hashimoto, William M. Jolly, Stephen C. Piper, Compton J. Tucker, Ranga B. Myneni, and Steven W. Running (2003) : Climate-Driven Increases in Global Terrestrial Net Primary Production from 1982 to 1999, Sience, vol.300, p. 1560-1563.
17) Olson, J.S.,J.A. Watts and L.J. Allison (1983) ：Carbon in Live Vegetation of Major World Ecosystems, Report ORNL-5862, Oak Ridge National Laboratory, Oak Ridge, Tennessee, USA.
18) Chapman W. L., Walsh J. E. (1993): Recent variations of sea ice and air temperatures in high latitudes. Bulletin of the American Meteorological Society 74, 33–47
19) Makhinova A. (2003): Smoke from forest fires and innocent hostages to experiments with nature, Siberian Agreement Interregional Association, A quarterly political information and analytical illustrated magazine, No.2 (12), 47–52
20) Kondoh, Kaihotsu, Hitata and Dorgorsuren（2005）：Interannual Variation of Phenology and Biomass in Mongolian Herbaceous Vegetation, Journal of Arid Land Studies, 14(4) , 209-218, [in Japanese]
21) Kondoh, Tateishi, Runtunuwuand Park（2002）：Relating Vegetation Activity to Climatic Variation and Atmospheric CO2 Content, Japan Society of Hydrology and Water Resources, 15(2) , 128-13, [in Japanese]